CHEMISTRY OF MATERIALS
Article

Chem. Mater. **2009,** *21,* 3177–3182 3177
DOI:10.1021/cm900625w

Self-Reorganization of CdTe Nanoparticles into Near-Infrared $Hg_{1-x}Cd_xTe$ Nanowire Networks

Jie Yang,[†,‡] Yunlong Zhou,[†] Shanliang Zheng,[†] Xinfeng Liu,[†] Xiaohui Qiu,[†] Zhiyong Tang,*[,†] Rui Song,*[,‡] Yujian He,*[,‡] Chi Won Ahn,*[,§] and Jeoung Woo Kim*[,§]

[†]*National Center for Nanoscience and Technology, 11 Beiyitiao, ZhongGuanCun, Beijing, 100190, P.R. China,* [‡]*College of Chemistry and Chemical Engineering, Graduate University of Chinese Academy of Sciences, Shijingshan, Yuquan Road, 19 (A), Beijing, 100049, P.R. China, and* [§]*National NanoFab Center, Daejeon 305-806, Korea*

Received March 4, 2009. Revised Manuscript Received May 21, 2009

In this study a self-reorganization strategy is applied to prepare near-infrared $Hg_{1-x}Cd_xTe$ nanowire networks. CdTe nanoparticles (NPs) self-reorganized into $Hg_{1-x}Cd_xTe$ nanowire networks by taking advantage of the synergic effect of chemical replacement inside NPs and physical attraction between NPs. The dipole−dipole interactions play a vital role in the formation of the nanowire network structures. The near-infrared optical absorption of the nanowire networks is easily tailored in a broad region from 700 to 1200 nm by changing their composition. The $Hg_{1-x}Cd_xTe$ nanowire networks exhibit fast optoelectrical response and good stability under illumination with 785 nm laser. Not only is the disadvantage of charge carrier transport between nanoparticles overcome, but also the nanowire networks show simplicity and facility in the device fabrication procedure, which is important for their future application in optoelectronics.

Introduction

Utilization of inorganic nanoparticles (NPs) as the start units to fabricate advanced structures is of both scientific and practical importance.[1,2] Generally, the strategies involving in such fabrications can be divided into two categories. The first type of methods is the self-assembly of NPs into one-, two-, or three-dimensional nanostructures by taking advantage of physical interactions between NPs, for example, electrostatic interaction, Van der Waals force, hydrogen bonding, hydrophobic interaction, or dipole moment attraction.[3−8] Another type of methods is to control composition and structural changes of NPs by using classic chemical reactions, for example, synthesis, decomposition, or replacement.[9−12] Nevertheless, little attention is paid to *simultaneously* manipulating the chemical reactions inside NPs and physical interactions between NPs,[13] although such research will obviously help us to understand the physicochemical nature of NPs as well design the advanced nanostructures with well-defined functionality. In this paper, we report a self-reorganization strategy to synthesize near-infrared $Hg_{1-x}Cd_xTe$ nanowire networks with tunable band gaps. The chemical replacement of CdTe NPs with Hg^{2+} ions is used to control composition of $Hg_{1-x}Cd_xTe$, and meanwhile the physical consequences of dipole−dipole forces between NPs give rise to production of nanowire network structures.

Alloy $Hg_{1-x}Cd_xTe$ as a typical narrow gap semiconductor has been extensively used in near-infrared optoelectronic devices, such as laser, light emitting diodes, photodetectors, and photovoltaics,[14−16] owing to its unique properties: (1) very similar lattice constants of HgTe and CdTe, only 0.3% lattice mismatch, leading to facile formation of $Hg_{1-x}Cd_xTe$ structures, and (2) remarkable difference in band gap of HgTe and CdTe, 1.6 eV for CdTe and about 0 eV for HgTe, leading to a tunable band gap of $Hg_{1-x}Cd_xTe$ in a wide infrared region.[17,18] The

*Corresponding authors. E-mail: zytang@nanoctr.cn (Z.T.); rsong@gucas.ac.cn (R.S.); heyujian@gucas.ac.cn (Y.H.); cwahn@nnfc.com (C.W.A.); jwkim@nnfc.com (J.W.K.).

(1) Murray, C. B.; Kagan, C. R.; Bawendi, M. G. *Annu. Rev. Mater. Sci.* **2000**, *30*, 545.
(2) Kotov, N. A. Nanoparticle Assemblies and superstructures; Marcel Dekker: New York, 2005.
(3) Tang, Z.; Kotov, N. A.; Giersig, M. *Science* **2002**, *297*, 237.
(4) Tang, Z.; Zhang, Z.; Wang, Y.; Glotzer, S. C.; Kotov, N. A. *Science* **2006**, *314*, 274.
(5) Murray, C. B.; Kagan, C. R.; Bawendi, M. G. *Science* **1995**, *270*, 1335.
(6) Sherchenko, E. V.; Talapin, D. V.; Kotov, N. A.; Brien, S. O.; Murray, C. B. *Nature* **2006**, *439*, 55.
(7) Tao, A.; Sinsermsuksakal, P.; Yang, P. *Nat. Nanotechnol.* **2007**, *2*, 435.
(8) Döllefeld, H.; Weller, H.; Eychmüller, A. *J. Phys. Chem. B* **2002**, *106*, 5604.
(9) Sun, Y.; Xia, Y. *J. Am. Chem. Soc.* **2004**, *126*, 3892.
(10) Son, D. H.; Hughes, S. M.; Yin, Y.; Alivisatos, A. P. *Science* **2004**, *306*, 1009.
(11) Robinson, R. D.; Sadtler, B.; Demchenko, D. O.; Erdonmez, C. K.; Wang, L.; Alivisatos, A. P. *Science* **2007**, *317*, 355.
(12) Mokari, T.; Rothenberg, E.; Popov, I.; Costi, R.; Banin, U. *Science* **2004**, *304*, 1787.
(13) Tang, Z.; Podsiadlo, P.; Shim, B. S.; Lee, J.; Kotov, N. A. *Adv. Func. Mater.* **2008**, *18*, 3801.
(14) Rogalski, A. *Rep. Prog. Phys.* **2005**, *68*, 2267.
(15) Allgaier, R. S. *J. Opt. Technol.* **1996**, *63*, 804.
(16) Rogach, A. L.; Eychmüller, A.; Hickey, S. G.; Kershaw, S. V. *Small* **2007**, *3*, 536.
(17) Balcerak, R.; Gibson, J. F.; Guiterrez, W.; Pollard, J. H. *Opt. Eng.* **1987**, *26*, 191.
(18) Rath, S.; Sahu, S. N. *Surf. Sci.* **2006**, *600*, L110.

Published on Web 06/29/2009

first examples of $Hg_{1-x}Cd_xTe$ NPs with tunable emission in the near-infrared region between 800 and 1100 nm were synthesized through partial chemical replacement of Cd^{2+} ions in the prepared CdTe NPs with Hg^{2+} ions.[19−21] Following the above work, other types of $Hg_{1-x}Cd_xTe$-based nanomaterials, for example, $Hg_{1-x}Cd_xTe$/CdS or $Hg_{1-x}Cd_xTe$/ZnS core/shell NPs and $Hg_{1-x}Cd_xTe$ nanorods, were also prepared.[22−24] Until now the shapes of the obtained $Hg_{1-x}Cd_xTe$ nanomaterials are only particles or rods with small aspect ratios, whereas one-dimensional nanowires with large aspect ratios are known as the key building blocks in nanodevices.[25−28]

Experimental Section

(1) Materials. Cadmium perchlorate hexahydrate ($Cd(ClO_4)_2 \cdot 6H_2O$), mercury perchlorate trihydrate ($Hg(ClO_4)_2 \cdot 3H_2O$), 2-aminoethanethiol hydrochloride ($HSCH_2CH_2NH_2$, 98+%), aluminum telluride (Al_2Te_3, 99.5%), sulfuric acid (H_2SO_4, 99%), and sodium hydroxide (NaOH, 98%) were purchased from Alfa Aesar. 2-Propanol ($CH_2CH(OH)CH_2$, HPLC) was purchased from Aldrich. All chemicals were used as received without further purification.

(2) Synthesis of MEA-Capped CdTe NPs. A solution of 0.496 g (1.18 mmol) of $Cd(ClO_4)_2 \cdot 6H_2O$ and 0.324 g (2.85 mmol) of 2-aminoethanethiol hydrochloride (MEA) in 62 mL of ultrapure water was adjusted to pH 5.0 with 1 M NaOH. The solution was placed in a three-necked flask and was deaerated by N_2 bubbling for about 30 min. H_2Te gas (generated by the reaction of 0.1 g of Al_2Te_3 and 10 mL of 0.5 M H_2SO_4 under N_2 atmosphere) was passed through the solution together with a slow nitrogen flow. Under stirring, the system was heated at 100 °C for 6 h. The final products were MEA-stabilized CdTe NPs with a maximum emission at 575 nm.

(3) Preparation of $Hg_{1-x}Cd_xTe$ Nanowire Networks. The MEA stabilizers of CdTe NPs were partially removed by isopropanol through centrifugation (12 000 rpm for 10 min). Subsequently, the precipitate was redissolved into Hg^{2+} solutions with different concentrations of 1.0 mM, 2.0 mM, 5.0 mM, 7.5 mM, and 10.0 mM, respectively. The final concentrations of CdTe molecules from NPs in all solutions were fixed to 2.5 mM, and pH values of all solutions were adjusted to 5.0. The solutions were bubbled with N_2 gas for 10 min to remove any dissolved oxygen and then kept at room temperature in the dark for 3 days. Finally, $Hg_{1-x}Cd_xTe$ nanowire networks precipitated from the solutions were collected and washed with ultrapure water several times.

(4) Characterization. Photoluminescence (PL) spectra were measured using Fluoromax-4 Spectrofluorometer (Japan). UV−vis absorption spectra were recorded on a Lambda 950 UV−visible spectrophotometer (Perkin-Elmer Inc., U.S.A.). The powder XRD patterns were recorded with a D/max2500 X-ray powder diffractometer (Japan). The sizes and the morphologies of the samples were observed using scanning electron microscopy S-4800 (HITACHI, Japan) and transmission electron microscopy Tecnai G^2 20 (FEI, U.S.A.). Energy dispersive X-ray (EDX) spectra were also recorded by EDAX (U.S.A.). The elemental compositions were measured by X-ray photoelectron spectroscopy ESCALab220I (Japan).

(5) Photoelectric Measurements. Interdigitated finger-like Ti/Au electrodes on silica substrates were purchased from Institute of Semiconductor, Chinese Academy of Sciences. The interelectrode spacing was 5 μm, and the number of periods was 50. The $Hg_{1-x}Cd_xTe$ nanowire networks in 2 μL solution were carefully and homogenously deposited onto the top of the metallic electrodes. The films were then annealed at 150 °C for 2 h in vacuum for drying. SEM observations showed that the annealing process did not change the nanowire network structures. The $I-V$ characteristics and the corresponding optoelectric properties of nanowire networks were performed on Keithley 4200-SCS with a two-probe system. All the measurements were operated at room temperature and under ambient conditions. For the dark current measurements, the devices were placed inside an optically sealed and electrically shielded box. The photocurrents were measured under illumination by a near-infrared laser with a wavelength of 785 nm.

Results and Discussion

Water-soluble, 2-aminoethanethiol (MEA)-stabilized CdTe NPs with a photoluminescence (PL) peak at 575 nm were used as starting units for self-reorganization process (Figure S1A in Supporting Information). If the Hg^{2+} ions were directly added into the prepared CdTe NP solution without any pretreatment, the transformation products were $Hg_{1-x}Cd_xTe$ NPs (Figure S2 in Supporting Information). This result is consistent with previous observation on a simple chemical replacement of Cd^{2+} ions in CdTe NPs with Hg^{2+} ions, which is facilitated by the lower solubility of HgTe in water relative to CdTe and gives rise to the production of $Hg_{1-x}Cd_xTe$ NPs.[21]

Simultaneous unitization of chemical replacement inside NPs and physical attractions between NPs is realized by adopting CdTe NPs with partial removal of stabilizers, also called stabilizer-depleted NPs, as reactants.[29] The partial removal of MEA stabilizers was performed by precipitating CdTe NPs from the crude solution via the method of antisolvent/centrifugation (see Experimental Section for details). Characterization results revealed that, after partial removal of MEA stabilizers, CdTe NPs remained almost unchanged with diameters of around 3.3 nm and a face centered cubic (FCC) crystal structure (Figure S1A,B in Supporting Information), whereas the density of MEA stabilizers on the NP surface was estimated to decrease from original 0.9 monolayers to 0.3 monolayers (Figure S1C,D in Supporting Information).[30] The stabilizer-depleted CdTe

(19) Kershaw, S. V.; Burt, M.; Harrison, M.; Rogach, A. L.; Weller, H.; Eychmüller, A. *Appl. Phys. Lett.* **1999**, *75*, 1694.
(20) Harrison, M. T.; Kershaw, S. V.; Burt, M. G.; Eychmüller, A.; Weller, H.; Rogach, A. L. *Mater. Sci. Eng., B* **2000**, *69*, 355.
(21) Rogach, A. L.; Harrison, M. T.; Kershaw, S. V.; Kornowski, A.; Burt, M. G.; Eychmüller, A.; Weller, H. *Phys. Status Solidi* **2001**, *224*, 153.
(22) Qian, H.; Dong, C.; Peng, J.; Qiu, X.; Xu, Y.; Ren, J. *J. Phys. Chem. C* **2007**, *111*, 16852.
(23) Tsay, J. M.; Pflughoefft, M. L.; Bentolila, A.; Weiss, S. *J. Am. Chem. Soc.* **2004**, *126*, 1926.
(24) Tang, B.; Yang, F.; Lin, Y.; Zhuo, L.; Ge, J.; Cao, L. *Chem. Mater.* **2007**, *19*, 1212.
(25) Kim, D. W.; Cho, K.; Kim, H.; Moon, B. M.; Kim, S. *Microelectron. Eng.* **2007**, *84*, 1643.
(26) Sun, Y.; Rogers, J. A. *J. Mater. Chem.* **2007**, *17*, 832.
(27) Sun, Y.; Choi, W. M.; Jiang, H.; Huang, Y. Y.; Rogers, J. A. *Nat. Nanotechnol.* **2006**, *1*, 201.
(28) Milliron, D. J.; Hughes, S. M.; Cui, Y.; Manna, L.; Li, J. B.; Wang, L. W.; Alivisatos, A. P. *Nature* **2004**, *430*, 190.
(29) Tang, Z.; Wang, Y.; Shanbhag, S.; Kotov, N. A. *J. Am. Chem. Soc.* **2006**, *128*, 6730.
(30) Bailey, R. E.; Strausburg, J. B.; Nie, S. *J. Nanosci. Nanotechnol.* **2004**, *4*, 569.

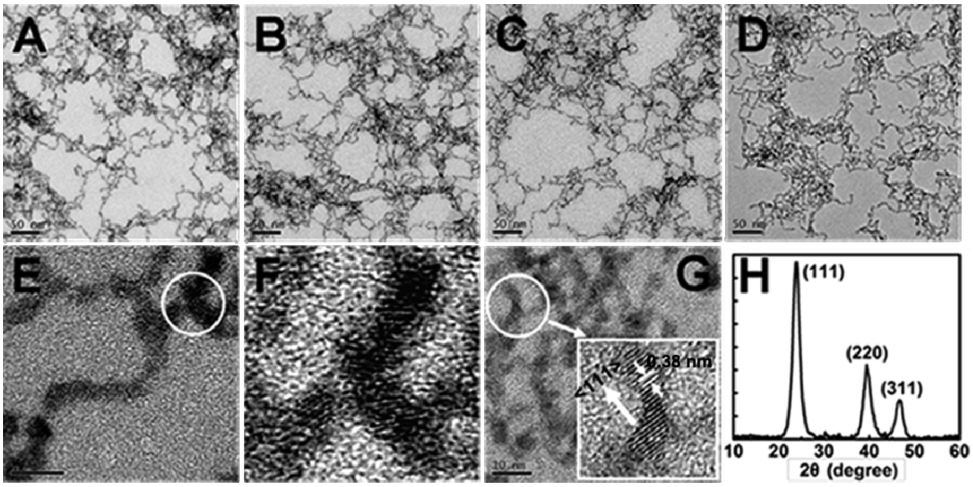

Figure 1. Transmission electron microscopy (TEM) images of $Hg_{1-x}Cd_xTe$ nanowire networks: (A) $Hg_{0.79}Cd_{0.21}Te$, (B) $Hg_{0.92}Cd_{0.08}Te$, (C) $Hg_{0.96}Cd_{0.04}Te$, and (D) $Hg_{0.97}Cd_{0.03}Te$. (E−G) High resolution transmission electron microscopy (HRTEM) images of $Hg_{0.92}Cd_{0.08}Te$ nanowire networks. (F) The enlarged HRTEM image for the circled area of interconnection parts from (E). The inset in (G) represents the single-crystalline structure of the nanowires. (H) Powder X-ray diffraction (XRD) pattern of $Hg_{0.92}Cd_{0.08}Te$ nanowire networks.

NP precipitates were then redissolved in $Hg(ClO_4)_2$ solutions with varying concentration at pH 5.0, and the final concentration of CdTe molecules from NPs in all solutions was fixed to 2.5 mM. Regardless of the concentration of $Hg(ClO_4)_2$, brown precipitates appeared after the mixed solution of Hg^{2+} ions, and the stabilizer-depleted CdTe NPs were kept under ambient conditions for three days. The brown precipitates were taken out and dispersed in pure water for subsequent characterizations and measurements.

Transmission electron microscopy (TEM) images indicate that all cation exchange products of the stabilizer-depleted CdTe NPs are nanowire networks when the concentrations of $Hg(ClO_4)_2$ in mixture solutions vary from 2.0 mM to 10.0 mM (Figure 1A−D). Close observation of the nanowire networks can tell us two important features: (1) the nanowires have identical diameters of 3.3 ± 0.2 nm with a rather narrow distribution, no matter in the same networks or in the networks that were prepared using $Hg(ClO_4)_2$ solutions with different concentration (Figure 1A−D), and (2) the interconnection parts of the crystalline nanowires are mostly present in dislocations, as shown in high resolution transmission electron microcopy (HRTEM) images (Figure 1E−F), while the nanowires present single-crystalline structure with a preferential growth direction along [111] (inset in Figure 1G). Large-scale scanning electron microscope (SEM) images further show that these nanowire networks extend to form relatively homogeneous thin films (Figure S3 in Supporting Information), which benefit their potential applications in devices.

Structural analysis by X-ray diffraction (XRD) suggests that all nanowire networks belong to the identical FCC system with three dominant peaks (111), (220), and (311) (Figure 1H and Figure S4 in Supporting Information). The lattice parameters of nanowire network match very well with those of CdTe (Fcc, $F\bar{4}3m$, a = 6.481 Å) and HgTe (Fcc, $F\bar{4}3m$, a = 6.460 Å), which provide the indirect evidence of the $Hg_{1-x}Cd_xTe$ nature of nanowire networks. It should be pointed out that the nanowire network structures are obtained from solutions of 2.5 mM CdTe mixed with $Hg(ClO_4)_2$ in the range of concentrations from 2.0 mM to 10.0 mM. When the concentration of $Hg(ClO_4)_2$ in a solution of pH 5.0 is higher than 10.0 mM, it is easily hydrolyzed to form insoluble $Hg(OH)_2$. On the other hand, when the concentration of $Hg(ClO_4)_2$ is lowered to 1.0 mM, the obtained product is the mixture of nanowires and nanopheres with an average diameter of about 50 nm (Figure S5 in Supporting Information). Elemental analysis results show that the compositions of nanospheres are also Hg, Cd, and Te, which can be substantiated further by XRD survey, in which three diffraction peaks are indexed to FCC $Hg_{1-x}Cd_xTe$ (Figure S5 in Supporting Information). Nevertheless, our study shown here focused on $Hg_{1-x}Cd_xTe$ nanowire networks.

The composition of $Hg_{1-x}Cd_xTe$ nanowire networks is further obtained by X-ray photon spectroscopy (XPS) survey (Table 1). The nanowire networks, which are cation exchange products of CdTe NPs with 2.0 mM, 5.0 mM, 7.5 mM, and 10.0 mM of Hg^{2+}, can be assigned to $Hg_{0.79}Cd_{0.21}Te$, $Hg_{0.92}Cd_{0.08}Te$, $Hg_{0.96}Cd_{0.04}Te$, and $Hg_{0.97}Cd_{0.03}Te$, respectively. It is not surprising that the content of Hg in $Hg_{1-x}Cd_xTe$ nanowire networks increases with the concentration of Hg^{2+} in reaction solution. On the other hand, the replacement of Cd^{2+} by Hg^{2+} in nanostructures is not 100% even though the Hg^{2+} amount is a large excess amount compared with Cd^{2+} (10.0 mM vs 2.5 mM). Since the cation exchange reactions start from CdTe NP surfaces, the gradient formation of $Hg_{1-x}Cd_xTe$ shells makes the subsequent replacement of CdTe inside with Hg^{2+} more and more difficult, which prevents complete replacement of Cd^{2+} by Hg^{2+} in nanostructures.[20,21] Nevertheless, the composition of $Hg_{1-x}Cd_xTe$ nanowire networks can be controlled by changing the concentration of Hg^{2+} in the reaction solution.

The above observations confirm that, besides chemical replacement with Hg^{2+}, the stabilized-depleted CdTe NPs

Table 1. Elemental Composition of the $Hg_{1-x}Cd_xTe$ Nanowire Networks Calculated from X-ray Photon Spectroscopy (XPS) Data

initial C_{Hg}^{2+} (mmol)	elemental composition[a] Te (%)	Cd (%)	Hg (%)	chemical formula
2.0	46.8 ± 1.7	11.1 ± 0.4	42.1 ± 0.9	$Hg_{0.79}Cd_{0.21}Te$
5.0	49.9 ± 0.6	3.8 ± 2.1	46.3 ± 0.7	$Hg_{0.92}Cd_{0.08}Te$
7.5	51.1 ± 0.5	1.5 ± 1.6	47.4 ± 1.3	$Hg_{0.94}Cd_{0.06}Te$
10.0	49.7 ± 1.8	1.5 ± 1.1	48.8 ± 0.8	$Hg_{0.97}Cd_{0.03}Te$

[a] The data of elemental composition were obtained from XPS measurements of Te 3d5 at 572.4 eV, Cd 3d5 at 405.2 eV, and Hg 4f7 at 100.1 eV.

encounter interparticle physical interactions, which give rise to production of nanowire network structures. Our and others' previous studies showed that partial removal of stabilizers from NP surfaces changed the physical interactions between NPs; that is, it decreased the electrostatic repulsion from stabilizers and meanwhile increased dipole attraction from NP cores. The exposed dipole attraction, which was strong enough to counteract electrostatic repulsion between NPs and overcame the random Brownian motion of NPs, forced the stabilizer-depleted NPs to self-align into one-dimensional (1D) chains, nanowires, or branched nanowire networks.[3,31−35] In the case of Hg-replaced CdTe NPs, the dipole attractions result in self-reorganization of the stabilizer-depleted NPs into 1D nanowires, and simultaneously high-energy defects of NPs or nanowires produced in either removal of partial stabilizers or the chemical replacement process (inset in Figure 1E) make NPs or nanowires spontaneously attach each other to form branched structures. Therefore, the nanowire networks are produced by controlling the above driving forces. The TEM image of the intermediate state also proves that $Hg_{1-x}Cd_xTe$ can form the branched nanorod structures before developing into nanowire networks (Figure S6 in Supporting Information). In contrast, without removal of stabilizers, the abundant MEA stabilizers and corresponding electrostatic repulsions screen both the dipole interactions and surface defects. Thus, $Hg_{1-x}Cd_xTe$ NPs are obtained with direct addition of Hg^{2+} into the crude solution of CdTe NPs (Figure S2 in Supporting Information).

The near-infrared optical properties of $Hg_{1-x}Cd_xTe$ nanowire networks are studied by investigating their absorption spectra (Figure 2). Impressively, nanowire networks exhibit strong absorption characteristics in the near-infrared region from 700 to 1200 nm, and the absorption peak positions of nanowire networks vary with the composition of Hg and Cd in the $Hg_{1-x}Cd_xTe$ system. Since the nanowires in the networks have similar diameters of 3.3 nm, the different positions of absorption

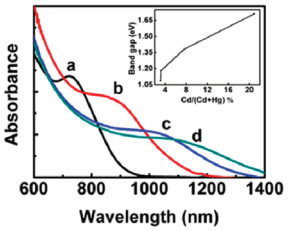

Figure 2. Room-temperature optical absorption spectra of near-infrared $Hg_{1-x}Cd_xTe$ nanowire networks: (a) $Hg_{0.79}Cd_{0.21}Te$, (b) $Hg_{0.92}Cd_{0.08}Te$, (c) $Hg_{0.96}Cd_{0.04}Te$, and (d) $Hg_{0.97}Cd_{0.03}Te$. The inset shows the band gap against the ratio of Cd in the alloy structures.

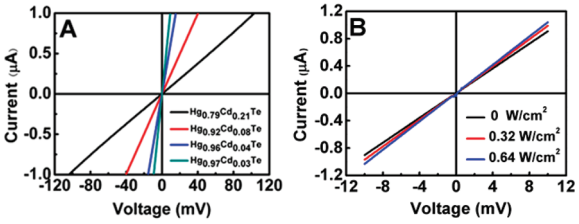

Figure 3. (A) $I-V$ curves of $Hg_{1-x}Cd_xTe$ nanowire networks measured at room temperature without illumination; (B) $I-V$ curves of alloy $Hg_{0.97}Cd_{0.03}Te$ nanowire networks measured at room temperature under light irradiation of varying intensity at 785 nm.

peaks are mainly ascribed to band gap modulation caused by the difference in nanowires' compositions rather than sizes. The band gap energy of the nanowire networks can be estimated from the absorption edge values in Figure 2, and the relationship between the band gap and the Cd content in alloy nanowires is plotted (inset in Figure 2). The band gap of nanowire networks narrows with the decrease of the x value in $Hg_{1-x}Cd_xTe$, which is consistent with the fact that the band gap of CdTe is much larger than that of HgTe. It is also noticed that, unlike bulk alloy, the change of band gap of $Hg_{1-x}Cd_xTe$ nanowire networks is not linear with the change of their composition (inset in Figure 2).[36] The different features of the composition-dependent band gap are most likely to originate from different elemental distributions inside the materials. Cd and Hg are homogenously distributed in bulk $Hg_{1-x}Cd_xTe$ alloy, whereas Hg and Cd are rich in the shells and cores of nanowires, respectively, due to gradual surface replacement of CdTe NPs with Hg^{2+}. Aside from the red shift of the exciton peaks, the broadened peak is another character of the absorption spectra. It is reasonable that many surface defects may be produced during gradual replacement and the self-assembly process, and meanwhile the wave functions are possibly distorted by the influence of surface charges.[34] Furthermore, the near-IR photoluminescence spectra of $Hg_{1-x}Cd_xTe$ nanowire networks are also measured, and unfortunately there are no photoluminescence features to be observed. The most likely reason is that the surface defects in $Hg_{1-x}Cd_xTe$ nanowires can quench the photoluminescence effectively.

(31) Volkov, Y.; Mitchell, S.; Gaponik, N.; Rakovich, Y. P.; Donegan, J. F.; Kelleher, D.; Rogach, A. L. *ChemPhysChem* **2004**, *5*, 1600.
(32) Rakovich, Y. P.; Volkov, Y.; Sapra, S.; Susha, A. S.; Döblinger, M. J.; Donegan, F.; Rogach, A. L. *J. Phys. Chem. C* **2007**, *111*, 18927.
(33) Gao, X.; Xing, G.; Chu, W.; Liang, X.; Zhao, Y.; Jing, L.; Yuan, H.; Cui, Y.; Dong, J. *Adv. Mater.* **2008**, *20*, 1794.
(34) Tobias, H.; Dirk, V.; joshua, J. C.; Christina, G. C.; Martijin, M. W.; René, A. J. J. *Appl. Mater. Interfaces* **2009**, *1*, 244.
(35) Zhang, Q.; Liu, S.; Yu, S. *J. Mater. Chem.* **2009**, *19*, 191.
(36) Wu, J.; Walukiewicz, W.; Yu, K. M.; Shan, W.; Ager, J. W.; Haller, E. E.; Miotkowski, I.; Ramdas, A. K.; Su, C. H. *Phys. Rev. B* **2003**, *68*, 033206-1.

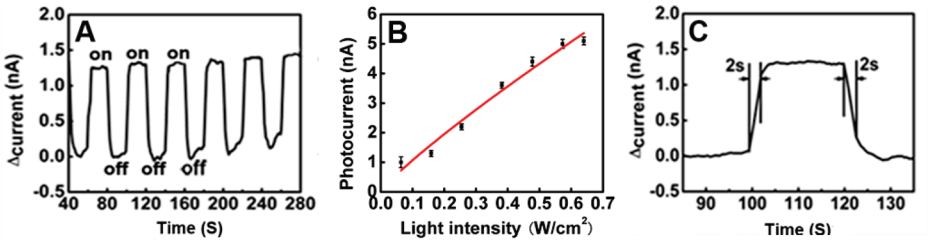

Figure 4. (A) Room-temperature time response of alloy $Hg_{0.79}Cd_{0.21}Te$ nanowire networks to the incidence light (785 nm, 0.16 W/cm^2), and the bias voltage applied is 10 mV. (B) The photocurrent versus the light intensity, and the red dashed line is a linear fitted curve. (C) Enlarged plot of (A); both the rise time and fall time are measured to be 2 s, respectively.

The nanowire networks with extended structures (Figure 1 and Figure S3 in Supporting Information) offer us an opportunity to interface nanomaterials with microscale or macroscale platforms. As an example, the nanowire networks were simply deposited onto the interdigitated finger-like electrodes for electrical measurement. The $I-V$ measurements were performed by using a two-probe method. Figure 3A shows typical $I-V$ curves of $Hg_{1-x}Cd_xTe$ nanowire networks measured in the dark. The resistance values measured from $I-V$ curves are 105.5 ± 2.5 KΩ, 40.5 ± 1.8 KΩ, 15.3 ± 1.6 KΩ, and 10.8 ± 0.8 KΩ for alloy $Hg_{0.79}Cd_{0.21}Te$, $Hg_{0.92}Cd_{0.08}Te$, $Hg_{0.96}Cd_{0.04}Te$, and $Hg_{0.97}Cd_{0.03}Te$ nanowire networks, respectively. It is easily understood that $Hg_{1-x}Cd_xTe$ nanowire networks with small x value have narrow band gaps, giving rise to low resistance and high conductance. In brief, both the optical and the electrical properties of $Hg_{1-x}Cd_xTe$ nanowire networks can be controlled by altering their composition. The resistance of $Hg_{1-x}Cd_xTe$ nanowire networks is found to be sensitive to the irradiated light intensity. As shown in Figure 3B, the resistance of $Hg_{0.97}Cd_{0.03}Te$ nanowire networks decreases from 11.0 KΩ measured in the dark to 9.6 KΩ under irradiation of laser light at a wavelength of 785 nm and an intensity of 0.64 W/cm^2. The above-gap near-infrared excitation generates free charge carriers in $Hg_{0.97}Cd_{0.03}Te$ nanowire networks and thus leads to decrease of the resistance of the nanowire networks. The near-infrared photosensitivity of $Hg_{1-x}Cd_xTe$ nanowire networks encourages us to explore their potential applications as photodetectors.

Figure 4A shows the real-time response of the $Hg_{0.79}Cd_{0.21}Te$ nanowire network to the incidence of near-infrared laser light. Upon exposure of the nanowire networks to the laser light with a wavelength of 785 nm at the bias of 10 mV, the current increases by about 1.3 nA quickly. When the laser light is turned off, the current of the nanowire networks rapidly decreases to its original value. It is also observed that the baseline of the off current curve increases slightly with on/off cycles, which is likely a feature for semiconductors that the resistance decreases with increasing temperature owing to the localized thermal effect. Despite the phenomena mentioned above, we still observe that such on/off sensing cycles can be repeated at least several hundred times without changing the switching amplitude (Figure 4A). The good reversibility and reproducibility of nanowire networks upon photoswitching will benefit their application as the near-infrared photodetectors.

The photoconductance is highly dependent on the incident light intensity. The simple power law dependence as given below can be applied to fit the relation of photocurrent (I) vs light intensity (P)

$$I = AP^{\theta}$$

where A is a constant and the exponent θ determines the response of photocurrent to light intensity. Figure 4B shows that the experimental data can be well fitted to the curve with a θ value of 0.87. The nonlinear photoconductance dependence on light intensity is attributed to the defect mechanisms.[37] As the light intensity increases, more recombination centers participate in the recombination process, which results in the gradual decrease of carrier lifetime and the slow increase of photocurrent. On the other hand, more free carriers are trapped by the exponentially distributed traps during the diffusion process of photoexcited carriers.

The response speed is another key parameter to determine the capability of a photodetector to track a fast-varying optical signal. Taken from Figure 4A, Figure 4C amplifies one on/off cycle of the $Hg_{1-x}Cd_xTe$ nanowire networks. Close examination reveals that the switching time of the $Hg_{1-x}Cd_xTe$ nanowire networks is about 2 s for both the rise and the fall time. The fast response of nanowire networks comes from their unique structures. In addition to high specific surface area, the nanowires cross-link with each other in the networks, which facilitate the carrier transfer in the interior of networks. Furthermore, multiple contacts between the nanowires and the electrodes also benefit the fast charge separation of nanowire networks. Note that the preparation of single nanowire devices needs the careful patterning of the electrodes onto the single nanowire, which is costly and time-consuming. As a comparison, in our process the nanowire networks are directly deposited onto the commercially available interdigital electrodes for photoconductivity measurement, and the simple and cheap procedure allows us to explore the practical application of nanowire networks as photodetectors.[38−40]

(37) Meier, H. OrganicSemiconductors: Dark- and Photo-Conductivity of Organic Solids; Chemie GmbH: Weinheim, 1974.
(38) Mcdonlad, S. A.; Konstantatos, G.; Zhang, S.; Cyr, P. W.; Klem, E. J. D.; Levina, L.; Sargent, E. H. *Nat. Mater.* **2005**, *4*, 138.
(39) Konstantatos, G.; Howard, I.; Fischer, A.; Hoogland, S.; Clifford, J.; Klem, E.; Levina, L.; Sargent, E. H. *Nature* **2006**, *442*, 180.
(40) Konstantatos, G.; Clifford, J.; Lerina, L.; Sargent, E. H. *Nat. Photonics* **2007**, *1*, 531.

Conclusions

In conclusion, near-infrared $Hg_{1-x}Cd_xTe$ nanowire networks are prepared by the self-reorganization process of CdTe NPs induced by Hg^{2+}. The synergic effect of chemical replacement of Cd^{2+} in CdTe NPs with Hg^{2+} and dipole attractions between CdTe NPs results in the formation of $Hg_{1-x}Cd_xTe$ nanowire networks. The $Hg_{1-x}Cd_xTe$ nanowire networks show the composition-dependent absorption features in a broad near-infrared region from 700 to 1200 nm. Under irradiation of near-infrared laser light with a wavelength of 785 nm, the $Hg_{1-x}Cd_xTe$ nanowire networks exhibit fast switching speed and good repeatability. This work may open the doors toward an understanding of the physicochemical properties of NPs as well as developing novel nanostructures with desirable functionalities.

Acknowledgment. This work was supported by the 100-talent program of Chinese Academy of Sciences (Z.Y.T.), the National Science Foundation of China (20773033, Z.Y.T.), the National High-tech Research and Development Program (2007AA03Z302, Z.Y.T.), and the Korea Foundation for International Cooperation of Science & technology (KICOS) through a grant provided by the Korean Ministry of Education, Science & Technology (MEST) in 2008 (No. K200722000002−08B010000210).

Supporting Information Available: Characterizations of CdTe nanoparticles and cation exchange products with Hg^{2+} ions under different conditions. This material is available free of charge via the Internet at http://pubs.acs.org.